Analysis of double laser emission occuring in 1.55 m InAs-InP (113)B quantum dot laser

Analysis of the Double Laser Emission Occurring in 1.55-μm InAs–InP (113)B Quantum-Dot Lasers

Kiril Veselinov, *Student Member, IEEE*, Frédéric Grillot, *Member, IEEE*, Charles Cornet, Jacky Even, Alexander Bekiarski, Mariangela Gioannini, and Slimane Loualiche

***Abstract*—In this paper, a theoretical model based on rate equations is used to investigate static and dynamic behaviors of InAs–InP (113)B quantum-dot (QD) lasers emitting at 1.55 μm. More particularly, it is shown that two modelling approaches are required to explain the origin of the double laser emission occurring in QD lasers grown on both, GaAs and InP substrates. Numerical results are compared to experimental ones by using either a cascade or a direct relaxation channel model. The comparison demonstrates that when a direct relaxation channel is taken into account, the numerical results match very well the experimental ones and lead to a qualitative understanding of InAs–InP (113)B QD lasers. Numerical calculations for the turn-on delay are also presented. A relaxation oscillation frequency as high as 10 GHz is predicted which is very promising for the realization of directly modulated QD lasers for high-speed transmissions.**

***Index Terms*—Double emission, InP, quantum dots (QDs), rate equations.**

I. Introduction

WHILE optics has proven to be the most practical response to the high traffic rate demand for long-haul transmission, its extension to the metropolitan networks down to the home remains an open challenge. The implementation of optics at transmission rate where other technical solutions exist requires cost reduction. As a consequence, semiconductor lasers based on low-dimensional heterostructures, such as a quantum-dot (QD) laser, are very promising. Indeed, QD structures have attracted a lot of attention in the last decade since they exhibit many interesting and useful properties such as low threshold current [1], temperature insensitivity [2], chirpless behavior [3], and optical feedback resistance [4]. As a result, thanks to QD lasers, several steps toward cost reduction can be reached as improving the laser resistance to temperature fluctuation in order to remove temperature control elements (Peltier cooler), or designing feedback resistant laser for isolator-free transmissions and optics-free module. Most investigations reported in the literature deal with InGaAs QD grown on GaAs substrates [5], [6]. However it is important to stress that InGaAs–GaAs QD devices do not lead to a laser emission above 1.35 μm which is detrimental for long-haul optical transmission. In order to reach the standards of long-haul transmissions, 1.55-μm InAs QD lasers grown on InP substrate have been developed. More particularly it has been demonstrated that the use of the specific InP(113)B substrate orientation when combined with optimized growth techniques allows the growth of very small (4 nm high) and dense (up to 10^{11} cm^{-2}) QD structures [7]. Recent experimental studies conducted on these devices have shown that a second laser peak appears in the laser spectrum as increasing the injection power. This double laser emission is a common property found independently by different research groups both for InGaAs–GaAs as well as for InAs–InP systems [8]–[10]. The experimental results in [9] have shown a saturation and complete rollover of the first emission after the occurrence of the excited state threshold, while an increasing behavior for both lasing wavelengths has been observed for a InAs–InP (113)B QD laser [10]. The origin of the double emission has been explained by the finite ground state (GS) relaxation time using a cascade relaxation model which brings the GS emission to a constant value after the excited state (ES) threshold [11]. This approach has been also used to extract the dynamical properties of QD laser [12], while the complete rollover has been attributed to an asymmetry in the thermal population redistribution [13].

In this paper a numerical model based on rate equations is used to model the double laser emission, to analyze the light–current characteristic as well as the turn-on delay of the QD-laser. Although numerous theories about carrier dynamics have been reported on QD InGaAs–GaAs devices [14], [15], such calculations have never been conducted in the case of 1.55-μm InAs–InP (113)B QD lasers. The paper is organized as follows. In Section II, an accurate description of the rate equation model is proposed. More particularly, it is shown that a modification of the model presented in [11] is required to explain the behavior of the P–I characteristics when the double laser emission occurs in QD lasers grown on InP substrates. Thus, in Section III, numerical results are presented and compared to experimental ones by using either a cascade or a direct relaxation channel model. After calculating the evolution of photon numbers as a function of the injected current density, it is shown that numerical results confirm those previously observed for InAs–GaAs system.

Manuscript received March 16, 2007; revised May 3, 2007. This work was supported in part by the European Network of Excellence on Photonic Integrated Components and Circuits (ePIXnet), in part by the Self-Assembled semiconductor Nanostructures for new Devices in photonics and Electronics (SANDiE) network of excellence, and in part by the Centre Régional Francophone d'Ingénierie pour le Développement (CREFID).

K. Veselinov is with the Laboratoire d'Etude des Nanostructures à Semiconducteurs, UMR CNRS FOTON 6082, Institut National des Sciences Appliquées, 35043 Rennes Cedex, France and also with the Technical University of Sofia, Sofia-1000, Bulgaria (e-mail: kiril.veselinov@ens.insa-rennes.fr).

F. Grillot, C. Cornet, J. Even, and S. Loualiche are with the Laboratoire d'Etude des Nanostructures à Semiconducteurs, UMR CNRS FOTON 6082, Institut National des Sciences Appliquées, 35043 Rennes Cedex, France (e-mail: frederic.grillot@insa-rennes.fr; charles.cornet@ens.insa-rennes.fr; jacky.even@insa-rennes.fr; slimane.loualiche@insa-rennes.fr).

A. Bekiarski is with the Technical University of Sofia, Sofia-1000, Bulgaria (e-mail: aabbv@tu-sofia.bg).

M. Gioannini is with the Dipartamento di Elettronica, Politecnico di Torino, 10129 Torino, Italy (e-mail: mariangela.gioannini@polito.it).

Digital Object Identifier 10.1109/JQE.2007.902386

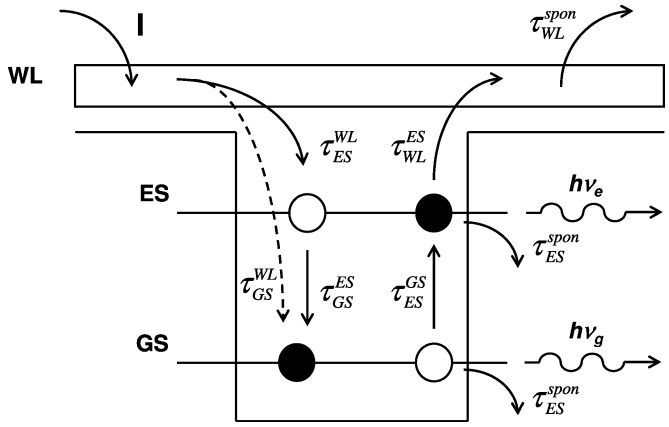

Fig. 1. Schematic representation of the carrier dynamics model with and without direct relaxation channel (dashed line).

On the other hand, it is also demonstrated that when a direct relaxation channel is taken into account, the numerical results match very well the different behavior of InAs–InP (113)B QD lasers, already published. In order to illustrate in more details the effect of the two-state lasing on the modulation properties of the InAs–InP (113)B QD laser, numerical calculations for the turn-on delay are also presented. For instance, a relaxation oscillation frequency as high as 10 GHz is predicted which is very suitable for high-speed transmissions. Finally, we summarize our results and conclusions in Section IV. Overall, this numerical investigation based on carrier dynamics is of prime importance for the optimization of low cost sources for optical telecommunications. Thanks to either a cascade relaxation model or an additional direct relaxation channel, the comparison between these two approaches leads to a qualitative understanding of the P–I characteristics in the two state lasing condition in 1.55-μm InAs–InP (113)B QD lasers.

II. Description of the Numerical Model

Numerical models based on rate equations are used to study carrier dynamics in the two lowest energy levels of an InAs–InP (113)B QD system. For simplicity the existence of higher excited states is neglected and a common carrier reservoir is associated to both wetting layer (WL) and barrier. It is assumed that there is only one QD ensemble, i.e., all dots have the same average size meaning that the inhomogeneous broadening enters in the differential gain parameter. The QD are assumed to be always neutral and electrons and holes are treated as electron–hole (eh)-pairs and thermal effects and carrier losses in the barrier region are not taken into account.

Fig. 1 shows a schematic representation of the carrier dynamics in the conduction band of a QD laser. First, an external carrier injection fills directly the WL reservoir with I being the injected current. Some of the eh-pairs are then captured on the fourfold degenerate ES of the QD ensemble with a capture time $\tau_{\rm ES}^{\rm WL}$ and some of them recombine spontaneously with a spontaneous emission time $\tau_{\rm ES}^{\rm spon}$. Once on the ES, carriers can relax on the twofold GS, be thermally reemitted in the WL reservoir or recombine spontaneously or by stimulated emission of photons with ES resonance energy. The same dynamic behavior is followed for the carrier population on the GS level with regard to the ES. This approach has been previously developed for the In(Ga)As–GaAs system [9] but in the case of InAs–InP (113)B system it is assumed that at low injection rates, the relaxation processes are phonon-assisted while the Auger effect dominates when the injection gets larger [16]. In order to include this effect, a modified model has been considered introducing a direct relaxation channel ($\tau_{\rm GS}^{\rm WL}$) to the standard cascade relaxation model as shown in Fig. 1 (dashed line). It is attributed to a single Auger process involving a WL electron captured directly into the GS by transferring its energy to a second WL electron [17]. Carriers are either captured from the WL reservoir into the ES or directly into the GS within the same time $\tau_{\rm GS}^{\rm WL} = \tau_{\rm ES}^{\rm WL}$. This assumption has been made after analysis of the kinetic curves in [16] where the ES and GS populations gave raise simultaneously 10 ps after excitation. On the other hand, carriers can also relax from the ES to the GS. The other transition mechanisms remain the same as in the previous model. The capture and the relaxation times are then calculated through a phenomenological relation depending on the carrier density in the WL reservoir [18]

$$\tau_{\rm GS}^{\rm ES} = \frac{1}{A_E + C_E N_W} \quad \tau_{\rm ES}^{\rm WL} = \frac{1}{A_W + C_W N_W} \tag{1}$$

where $\rm N_W$ is the carrier density in the WL reservoir and $A_W(A_E)$ and $C_W(C_E)$ are the coefficients for phonon and Auger-assisted relaxation, respectively, related to the WL and the ES. Their values have been experimentally estimated as follows: $A_W = 1.35\ 10^{10}\ \rm s^{-1}$, $C_W = 5\ 10^{-15}\ \rm m^3.s^{-1}$, $A_E = 1.5\ 10^{10}\ \rm s^{-1}$, $C_E = 9\ 10^{-14}\ \rm m^3.s^{-1}$ in a previous work [19]. The eh-pairs escape times have been derived considering a Fermi distribution for the ES and GS populations for the system in thermal equilibrium without external excitation [11]. Two rate-equation systems (RES) have been made, with and without direct relaxation channel describing the variation of the carrier numbers of the three electronic energy levels and the photon numbers in the cavity with ES and GS resonant energies

$$\frac{dN_{\rm WL}}{dt} = \frac{I}{e} + \frac{N_{\rm ES}}{\tau_{\rm WL}^{\rm ES}} - \frac{N_{\rm WL}}{\tau_{\rm ES}^{\rm WL}} f_{\rm ES} - \frac{N_{\rm WL}}{\tau_{\rm GS}^{\rm WL}} f_{\rm GS} - \frac{N_{\rm WL}}{\tau_{\rm WL}^{\rm spon}} \tag{2}$$

$$\frac{dN_{\rm ES}}{dt} = \frac{N_{\rm WL}}{\tau_{\rm ES}^{\rm WL}} f_{\rm ES} + \frac{N_{\rm GS}}{\tau_{\rm ES}^{\rm GS}} f_{\rm ES} - \frac{N_{\rm ES}}{\tau_{\rm WL}^{\rm ES}} - \frac{N_{\rm ES}}{\tau_{\rm GS}^{\rm ES}} f_{\rm GS} - \frac{N_{\rm ES}}{\tau_{\rm ES}^{\rm spon}} - N_B v_g a_{\rm ES} \left(\frac{N_{\rm ES}}{2N_B} - 1 \right) \frac{S_{\rm ES}}{1 + \varepsilon_{\rm ES} S_{\rm ES}} \tag{3}$$

$$\frac{dN_{\rm GS}}{dt} = \frac{N_{\rm WL}}{\tau_{\rm GS}^{\rm WL}} f_{\rm GS} + \frac{N_{\rm ES}}{\tau_{\rm GS}^{\rm ES}} f_{\rm GS} - \frac{N_{\rm GS}}{\tau_{\rm ES}^{\rm GS}} f_{\rm ES} - \frac{N_{\rm GS}}{\tau_{\rm GS}^{\rm spon}} - N_B v_g a_{\rm GS} \left(\frac{N_{\rm GS}}{N_B} - 1 \right) \frac{S_{\rm GS}}{1 + \varepsilon_{\rm GS} S_{\rm GS}} \tag{4}$$

$$\frac{dS_{\rm ES}}{dt} = N_B v_g a_{\rm ES} \left(\frac{N_{\rm ES}}{2N_B} - 1 \right) \frac{S_{\rm ES}}{1 + \varepsilon_{\rm ES} S_{\rm ES}} - \frac{S_{\rm ES}}{\tau_p} + \beta_{sp} \frac{N_{\rm ES}}{\tau_{\rm ES}^{\rm spon}} \tag{5}$$

$$\frac{dS_{\rm GS}}{dt} = N_B v_g a_{\rm GS} \left(\frac{N_{\rm GS}}{N_B} - 1 \right) \frac{S_{\rm GS}}{1 + \varepsilon_{\rm GS} S_{\rm GS}} - \frac{S_{\rm GS}}{\tau_p} + \beta_{sp} \frac{N_{\rm GS}}{\tau_{\rm GS}^{\rm spon}} \tag{6}$$

where $\rm N_{WL,ES,GS}$ are the populations in the WL reservoir, ES and GS. $\rm N_B$ is the total number of QD. $\rm S_{ES,GS}$ are the photon

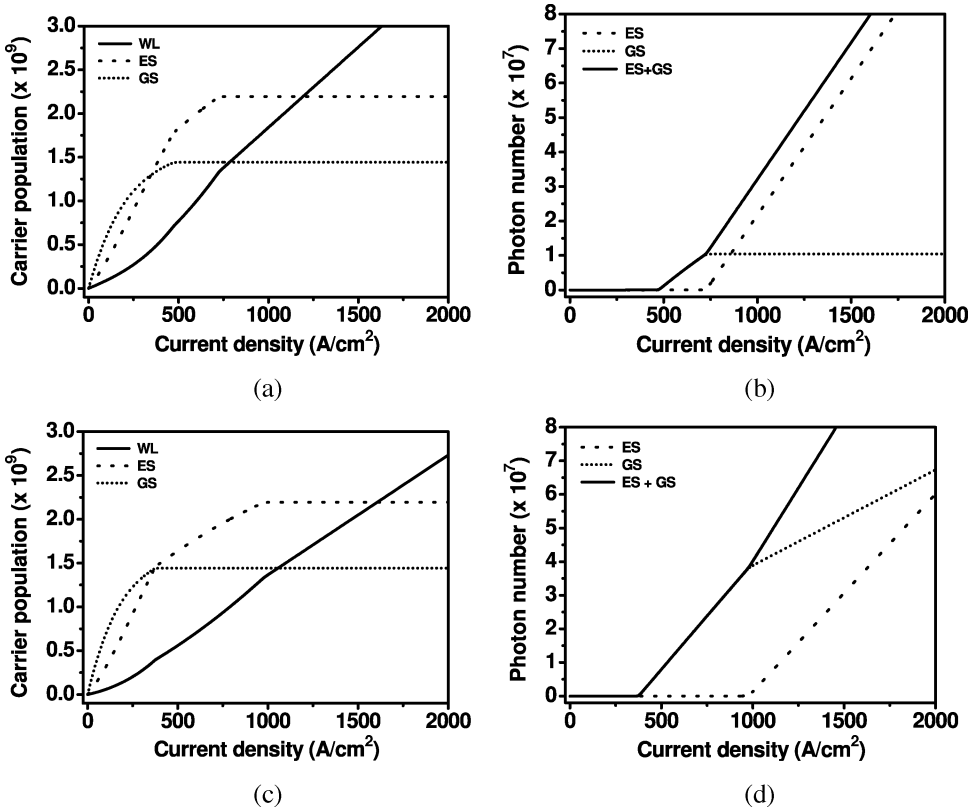

Fig. 2. Calculated level populations and photon number in the active region as a function of the injected current density for the (a)–(b) cascade relaxation model and (c)–(d) the direct relaxation channel model.

populations in the cavity with ES and GS resonant energy. Note that photons from S_{ES} and S_{GS} are assumed to be independent. $f_{ES,GS}$ are the probabilities to find an open seat for carriers, assuming fourfold and twofold degenerated ES and GS, respectively

$$f_{ES} = 1 - \frac{N_{ES}}{4N_B} \qquad f_{GS} = 1 - \frac{N_{GS}}{2N_B}. \tag{7}$$

The expression $\mp N_{WL} f_{GS}/\tau_{GS}^{WL}$ describing the relaxation from the WL to the GS has been neglected in the case of a standard cascade model in (2) and (4). The term $S_{ES,GS}/(1+\varepsilon_{ES,GS}S_{ES,GS})$, with $\varepsilon_{ES,GS}$ being the gain compression factor, represents the gain nonlinearities. In this work in order to stress the influence of the direct relaxation channel, $\varepsilon_{ES,GS}$ has been set to zero assuming linear gain variation. Furthermore the gain coefficients a_{ES} and a_{GS} in (3) to (6) have been used as adjustable parameters with $a_{GS} = a_{ES}/2.6$. The contribution of the ES and GS spontaneous emissions into the lasing mode is denoted by the coefficient β_{sp}. The photon lifetime is $\tau_p = 1/v_g[\alpha_i + \ln(1/R_1R_2)/(2L)]$, with $v_g = c/n_r$ being the group velocity, n_r the refractive index, α_i the internal loss, R_1 and R_2 the cavity mirror reflectivity, and L the laser length.

III. Results and Discussion

A. Numerical Steady-State Solutions

The steady-state solution is obtained by a numerical calculation of the RES for a linear increase of the injection current density. Fig. 2 presents results for the three carrier populations and the emitted photons in the laser cavity using the same simulation parameters for both cascade relaxation and direct channel models. In the first case Fig. 2(a)–(b), the results are similar with those already reported in the literature for the InAs–GaAs system [11]. Considering the carrier populations in Fig. 2(a) the ES exhibits a steady linear growth until GS reaches its lasing threshold and its population clamps at $1.4{\cdot}10^9$ while the ES continues with a decreased slope efficiency to reach the second lasing threshold and saturates at $2.2{\cdot}10^9$. For the photon numbers in the cavity, Fig. 2(b) a GS threshold current density of a 460 A/cm^2 has been estimated and once the second lasing of the ES appears at about 720 A/cm^2, the emission of the GS saturates completely and the ES emission increases linearly. These results confirm the theory of a two-state lasing competition between the GS and ES due to the finite GS relaxation time using the cascade relaxation model.

On the other hand, the RES with an additional direct relaxation channel shows a different behavior more suitable in the case of InAs–InP (113)B QD device due to a higher Auger assisted relaxation rate. Indeed, there is a slightly different carrier population characteristic, Fig. 2(c) where the ES growth is slower compared to the previous case and exhibits a smaller slope efficiency which applies also for the carriers in the WL. Although, the saturation values of the populations have not been changed the results for the photon numbers as a function of the injection current density are quite different. Fig. 2(d) shows two thresholds corresponding to the two laser emissions. When the ES stimulated emission appears at 970 A/cm^2, only a slight decrease of the GS slope efficiency is predicted. At the same time,

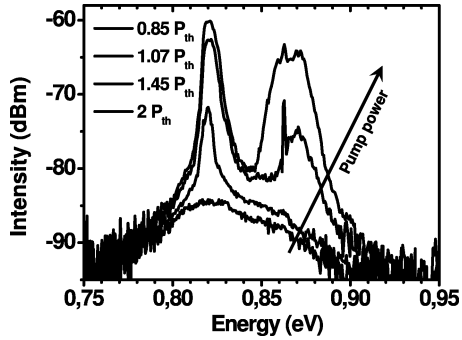

Fig. 3. Room-temperature emission spectra of a QD broad-area laser with six QD stacked layers (undoped structure) under a pulsed optical excitation of 0.85 Pth ($P\text{th} = 6.5$ kW cm $-$ 2), 1.07 Pth, 1.45 Pth, and 2 Pth from bottom to top of the figure, as reported in [10].

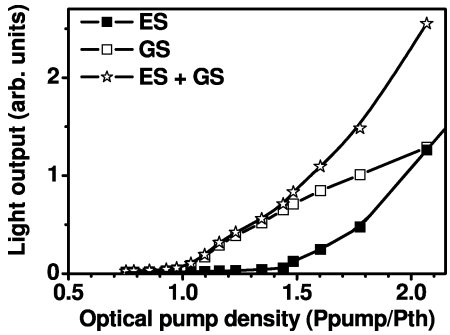

Fig. 4. Integrated light-output power versus optical normalised pumping density with respect to the GS threshold intensity.

TABLE I
SIMULATION PARAMETERS USED IN THE MODELS

Simulation parameters	
Active region length	L = 0.245 cm
Active region width	W = 0.012 cm
Number of QD layers	N = 6
QD surface density	$N_D = 5 \times 10^{10}$ cm^{-2}
Total number of QD	$N_B = 4.41 \times 10^9$
Internal modal loss	$\alpha_i = 6$ cm^{-1}
Mirror reflectivity	$R_1 = R_2 = 0.3$
Refractive index	$n_r = 3.27$
Spontaneous emission from WL	$\tau_{WL}^{spon} = 500\,ps$
Spontaneous emission from ES	$\tau_{ES}^{spon} = 500\,ps$
Spontaneous emission from GS	$\tau_{GS}^{spon} = 1200\,ps$
Spontaneous emission factor	$\beta_{sp} = 10^{-3}$

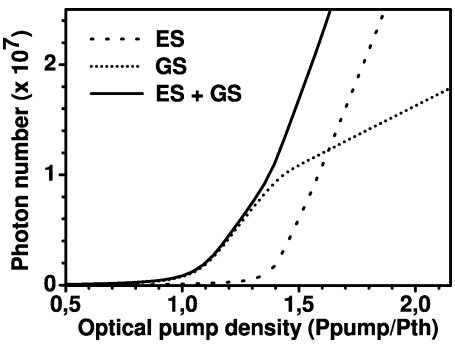

Fig. 5. Calculated photon number in the active region as a function of the normalised pump power with respect to the GS threshold intensity using the direct relaxation channel model.

the global slope efficiency increases. As a result, when a direct relaxation channel is taken into account, the difference between the two threshold currents (370 A/cm^2 for the GS) has almost doubled. Here, the double laser emission seems to result from the efficient carrier relaxation into the GS due to the pronounced single Auger process for larger injection rates [17]. Although the presence of nonlasing QD is not taken into account, it is shown in what follows that this numerical model gives a good qualitative understanding of the experimental results recently reported for an optical pumped InAs–InP (113)B diode laser [10].

B. Experimental Results

The studied laser whose structure has already been reported in [10] is composed of an active region with six InAs QD stacked layers. The cavity length is 2.45 mm with cleaved uncoated facets while the width of the strip is 120 μm. The optical pumped structure operates at room temperature under 1.06-μm pulsed excitation. The excitation pulse width is set at 13 ns with a repetition rate of 5 kHz. Fig. 3 shows the emission spectra as a function of the energy for different values of the pump power normalised with respect to the GS threshold value Pth. At low optical excitation (0.85 Pth), only spontaneous emission is measured. The peak is centred at 0.82 eV (1.51 μm) close to the peak maximum observed by conventional PL measurements. With increasing the optical excitation (1.07 Pth), laser emission occurs at 0.82 eV (1.51 μm). At threshold, the pumping power density is estimated to be 6.5 kW/cm^2. With increasing pumping power density the emission intensity increases. Then a second stimulated emission appears (above 1.45 Pth) centred at 0.87 eV (1.43 μm). The separation between the two emissions (50 meV) corresponds to the energy difference between the GS and the ES measured by time resolved photoluminescence on similar QD [16]. Fig. 4 shows integrated intensities of GS, ES and both emissions of the photoluminescence spectra under 1.06-μm pulsed excitation at RT. As it can be seen the measurement shows no GS clamping after the ES threshold is reached and a smooth transition from below to above threshold operation. In order to simulate this performance, the direct carrier relaxation model has been used and a broad area edge emitting laser has been assumed with the same structural parameters as the one used for the measurement. The simulation parameters are summarized in Table I, in agreement with [19] and [20].

The results from the simulation are given in Fig. 5 where the photon number in the laser cavity is presented as a function of the normalised pump power with respect to the GS threshold intensity to be comparable with the experimental data in Fig. 4. As the measured characteristic, the simulation results in no GS saturation and the ES and GS threshold currents are in the same range respectively. Taking into account the normalised pump intensity it is important to stress that this result, rather qualitative illustrates in a good matter the effect of the Auger assisted relaxation on the lasing performance. In this simulation the spontaneous emission factor β_{sp} has been adjusted to the value of 10^{-3} which is one order of magnitude bigger than the typical value of 10^{-4}. It is noteworthy, that the experimental P–I characteristics have been derived by integrating the laser spectra and

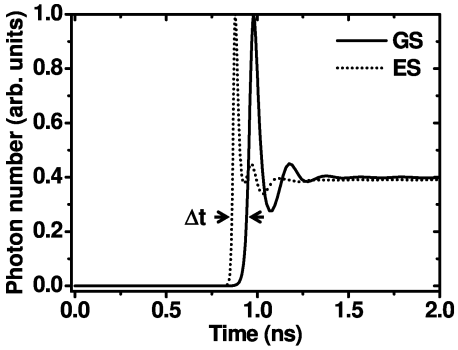

(a)

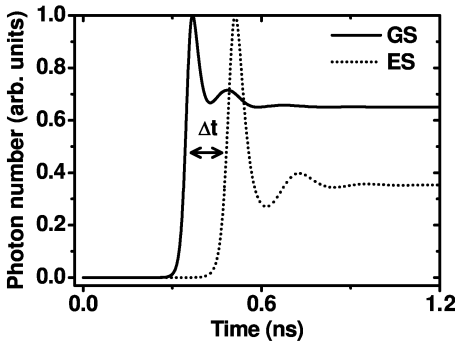

(b)

Fig. 6. Turn-on delays for the GS emission (solid line) and for the excited state emission (dot line) after a step-like current excitation for (a) the cascade relaxation model and (b) direct relaxation channel model.

that the RE model does not consider multimode laser emission. Thus, the actual spontaneous emission contribution to the lasing mode seems overestimated. However, it is a reasonable approximation in order to reproduce the smooth transition from below to above threshold operation shown on the experimental curves.

C. Turn-on Delay

Once the consistency of the direct carrier relaxation model has been demonstrated the same RES has been used to investigate the turn-on dynamics of the InAs–InP (113)B QD laser. In Fig. 6, the transient responses of the GS and ES, respectively, are shown for the two models, after introducing a step-like current pulse at time $t = 0$. Temporal evolution of photon numbers are traced by the fourth-order Runge–Kutta method. The system reaches the steady state after the relaxation oscillation. The magnitude of the current pulse has been chosen 2.7 times the ES threshold current of the direct carrier relaxation model [Fig. 2(d)] in order to investigate the system response in the proximity of the two-state lasing crossing point. In the case of the cascade relaxation model [Fig. 6(a)] the excitation intensity exceeds largely the crossing point of the ES and GS light–current characteristics. Therefore, the ES response appears first followed by the GS with time deviation $\Delta t = 88$ ps. The system reaches the steady state after relaxation oscillations (RO) as fast as $f_{\mathrm{RES}} = 12.8$ GHz for the ES and $f_{\mathrm{RGS}} = 5.2$ GHz for the GS. This result, predicting a wider modulation bandwidth for the ES compared to the GS is in agreement with previous work on InAs–GaAs QD lasers [12]. On the other hand in the case of the direct relaxation channel model, due to the greater threshold current difference and no GS saturation the system response is inverted and this time the ES characteristic follows the GS one with $\Delta t = 130$ ps [Fig. 6(b)]. It is shown that the GS trace exhibits a higher RO frequency ($f_{\mathrm{RGS}} = 9.0$)GHz compared to the ES trace ($f_{\mathrm{RES}} = 4.7$ GHz).

The simulations of the turn-on delay have been made using the same parameters for the two models and the same current in order to illustrate the effect of the direct channel on the laser response. On one hand, the turn-on delay of the system with direct channel is about three times shorter compared to the one of the cascade model. Since the carriers relax directly on the GS within the same time as those captured by the ES, an enhancement of the GS relaxation oscillation frequency by a factor of 1.7 is also observed. On the other hand, the more efficient the GS relaxation is, the more ES threshold increases. As a consequence, the ES relaxation oscillations decrease due to the lower above threshold excitation rate.

IV. Conclusion

In summary, the carrier level populations and photon numbers have been calculated versus the injected current density. Two modelling approaches have been used in order to investigate the origin of the double laser emission of a InAs–InP (113)B QD based laser. On one hand, numerical results describing carrier dynamic behavior have been presented confirming previously observed phenomena for InAs–GaAs system. On the other hand, it has been shown that the direct relaxation channel included in the model matches very well the different experimental results already published and leads to qualitative understanding of InAs–InP (113)B QD lasers. Also numerical results for the turn-on delay of the double laser emission have been presented exhibiting ROs frequency close to 10 GHz, which is suitable for high-speed transmissions. Next step to be done is to improve this numerical model by including the effect of the inhomogeneous broadening (QD size dispersion), the nonlinear gain variation and the multimode laser emission as well as to investigate the laser dynamic behavior under modulation. At the end, this numerical tool will be self-consistent and of first importance for the optimization of QDs based lasers and semiconductor optical amplifiers for long-haul applications.

Acknowledgment

The authors would like to thank Prof. I. Montrosset of Politecnico di Torino, Italy, for the critical reading of the manuscript and the useful and stimulating discussions.

References

[1] G. T. Liu, A. Stintz, H. Li, K. J. Malloy, and L. F. Lester, *Electron. Lett.*, vol. 35, pp. 1163–1165, 1999.

[2] S. S. Mikhrin, A. R. Kovsh, I. L. Krestnikov, A. V. Kozhukhov, D. A. Livshits, N. N. Ledentsov, Y. M. Shernyakov, I. I. Novikov, M. V. Maximov, V. M. Ustinov, and Z. I. Alferov, *Semicond. Sci. Technol.*, vol. 20, p. 340, 2005.

[3] H. Saito, K. Nishi, A. Kamei, and S. Sugou, *IEEE Photon. Technol. Lett.*, vol. 12, no. 10, pp. 1298–1300, Oct. 2000.

[4] D. O'Brien, S. P. Hegarty, G. Huyet, J. G. McInerney, T. Kettler, M. Laemmlin, D. Bimberg, V. M. Ustinov, A. E. Zhukkov, S. S. Mikhrin, and A. R. Kovsh, *Electron. Lett.*, vol. 39, no. 25, pp. 1819–1820, 2003.

[5] M. Grundmann, O. Stier, S. Bognar, C. Ribbat, F. Heinrichsdorff, and D. Bimberg, "Optical properties of self-organized quantum dots: Modelling and experiments," *Phys. Stat. Sol.*, vol. 178, p. 255, 2000.

[6] H. Hatori, M. Sugawara, K. Mukai, Y. Nakata, and H. Ishikawa, "Room-temperature gain and differential gain characteristics of self-assembled InGaAs–GaAs quantum dots for 1.1–1.3 μm semiconductor laser," *Appl. Phys. Let.*, vol. 77, no. 6, pp. 773–775, Aug. 2000.
[7] P. Caroff, C. Paranthoën, C. Platz, O. Dehaese, H. Folliot, N. Bertru, C. Labbé, R. Piron, E. Homeyer, A. LeCorre, and S. Loualiche, "High gain and low threshold InAs quantum dot lasers on InP," *Appl. Phys. Lett.*, vol. 87, pp. 243107–243107-3, Dec. 2005.
[8] M. Sugawara, N. Hatori, H. Ebe, Y. Arakawa, T. Akiyama, K. Otsubo, and Y. Nakata, "Modelling room-temperature lasing spectra of 1.3 μm selfassembled InAs–GaAs quantum-dot lasers: Homogeneous broadening of optical gain under current injection," *J. Appl. Phys.*, vol. 97, pp. 043523–043523-8, Jan. 2005.
[9] A. Markus, J. X. Chen, C. Paranthoen, A. Fiore, C. Platz, and O. Gauthier-Lafaye, "Simultaneous two-state lasing in quantum-dot lasers," *Appl. Phys. Let.*, vol. 82, no. 12, pp. 1818–1820, 2003.
[10] C. Platz, C. Paranthoen, P. Caroff, N. Bertru, C. Labbe, J. Even, O. Dehaese, H. Folliot, A. Le Corre, S. Loualiche, G. Moreau, J. C. Simon, and A. Ramdane, "Comparison of InAs quantum dot lasers emitting at 1.55 μm under optical and electrical injection," *Semicond. Sci. Technol.*, vol. 20, pp. 459–463, 2005.
[11] A. Markus, J. X. Chen, O. Gauthier-Lafaye, J. Provost, C. Paranthoën, and A. Fiore, "Impact of intraband relaxation on the performance of a quantum-dot laser," *IEEE J. Sel. Topics Quantum Electron.*, vol. 9, no. 5, pp. 1308–1314, Oct. 2003.
[12] M. Gioannini, A. Sevega, and I. Montrosset, "Simulations of differential gain and linewidth enhancement factor of quantum dot semiconductor lasers," *Opt. Quantum Electron.*, vol. 38, pp. 381–394, 2006.
[13] E. A. Viktorov, P. Mandel, Y. Tanguy, J. Houlihan, and G. Huyet, "Electron-hole asymmetry and two-state lasing in quantum dot lasers," *Appl. Phys. Lett.*, vol. 87, p. 053113, 2005.
[14] K. Mukai, Y. Nakata, K. Otsubo, M. Sugawara, N. Yokoyama, and H. Ishikawa, "1.3- μm CW lasing of InGaAs–GaAs quantum dots at room temperature with a threshold current of 8 mA," *IEEE Photon. Technol. Lett.*, vol. 11, no. 10, pp. 1205–1207, Oct. 1999.
[15] K. T. Tan, C. Marinelli, M. Thompson, A. Wonfor, M. Silver, R. Sellin, R. Penty, I. White, M. Lammlin, N. Ledentsov, D. Bimberg, A. Zhukov, V. Ustinov, and A. Kovsh, "High bit rate and elevated temperature data transmission using InGaAs quantum -dot lasers," *IEEE Photon. Technol. Lett.*, vol. 16, no. 5, pp. 1415–1417, May 2004.
[16] P. Miska, C. Paranthoen, J. Even, O. Dehaese, H. Folliot, N. Bertru, S. Loualiche, M. Senes, and X. Marie, "Optical spectroscopy and modelling of double-cap grown InAs–InP quantum dots with long wavelength emission," *Semicond. Sci. Technol.*, vol. 17, pp. L63–L67, 2002.
[17] B. Ohnesorge, M. Albrecht, J. Oshinowo, Y. Arakawa, and A. Forchel, "Rapid carrier relaxation in self-assembled $In_xGa_{1-x}As$–GaAs quantum dots," *Phys. Rev. B*, vol. 54, no. 16, pp. 11532–11538, Oct. 1996.
[18] T. Berg, S. Bischoff, I. Magnusdottir, and J. Mork, "Ultrafast gain recovery and modulation limitations in self-assemble quantum-dot devices," *IEEE Photon. Technol. Letters*, vol. 13, no. 6, pp. 541–543, Jun. 2001.
[19] K. Veselinov, F. Grillot, P. Miska, E. Homeyer, P. Caroff, C. Platz, J. Even, X. Marie, O. Dehaese, S. Loualicshe, and A. Ramdane, "Carrier dynamics and saturation effect in (311)B InAs–InP quantum dot lasers," *Opt. Quantum Electron.*, vol. 38, pp. 369–379, 2006.
[20] M. Sugawara, K. Mukai, Y. Nakata, and H. Ishikawa, "Effect of homogeneous broadening of optical gain on lasing spectra in self-assembled $In_xGa_{1-x}As$–GaAs quantum dot lasers," *Phys. Rev. B*, vol. 61, no. 11, pp. 7595–7603, 2000.
[21] C. Cornet, C. Labbé, H. Folliot, P. Caroff, C. Levallois, O. Dehaese, J. Even, A. Le Corre, and S. Loualiche, "Time-resolved pump probe of 1.55 μm InAs–InP quantum dots under high resonant excitation," *Appl. Phys. Let.*, vol. 88, pp. 171502–171502-3, Apr. 2006.

Kiril Veselinov (S'07) was born in Sofia, Bulgaria, in 1978. He received the M.S. degree in electrical engineering from Technical University of Sofia, Sofia, Bulgaria in 2002, where since 2004, he has been working toward the Ph.D. degree with the Francophone Department of Electrical Engineering, and also with the Department of Materials and Nanotechnology of National Institute of Applied Sciences of Rennes, France.

His research interests involve modeling and characterization of semiconductor lasers and optical amplifiers. Since 2004, his main research activity has been focused on modeling of quantum-dot materials and lasers.

Frédéric Grillot (M'02) was born in Versailles, France, in 1974. He received the M.Sc. degree in physics on light-matter interaction from the University of Dijon, Dijon, France, in 1999 and the Ph.D. degree in electrical engineering from the University of Besançon, Besançon, France, in 2003. His doctoral research activities conducted within Opto+, Alcatel Research & Innovation were on "monomode lasers with low feedback sensitivity for 2.5 Gb/s isolator-free transmissions."

From 2001 to 2003, he had a postdoctoral position at the Institut d'Electronique Fondamentale , Centre National de la Recherche Scientifique, University of Paris-Sud, France. His research activities were on integrated optics modelling and on Si-based passive devices for optical interconnects and telecommunications. Part of this work was also devoted to simulate scattering effects within submicron silicon-on-insulator (SOI) optical waveguides. In September 2004, he moved to the Institut National des Sciences Appliquées (INSA), Rennes, France where he is currently working as a lecturer within the Materials and Nanotechnologies (MNT) department. His main research activities are now focused on semiconductor quantum-dot lasers for low-cost applications.

Dr. Grillot is a Member of IEEE Lasers and Electro-Optics Society and la Société Française d'Optique.

Charles Cornet was born in Versailles, France, in 1978. He received the Ph.D. degree at the Institut National des Sciences Appliquées (INSA), Rennes, France, in 2006, working on quantum-dot lasers and fundamental properties.

He is now in a postdoctoral position in the Department of Nanomaterials and Nanotechnologies, INSA. His main field of activity is the study of the quantum dot growth and their optical properties for laser applications.

Jacky Even was born in Rennes, France, in 1964. He received the Ph.D. degree from the University of Rennes I, Rennes, France, in 1992.

He was a Research and Teaching Assistant, University of Rennes I, from 1992 to 1999. He has been Full Professor of Optoelectronics at the Institut National des Sciences Appliquées (INSA), Rennes, France, since 1999. His main field of activity is the theoretical study of the electronic, optical and nonlinear properties of QW and QD structures and the simulation of optoelectronic devices. He is author or coauthor of 80 papers.

Alexander Bekiarski was born in Plovdiv, Bulgaria, in 1944. He received the Ph.D. degree from the Technical University of Sofia, Sofia, Bulgaria, in 1975.

He was a Research and Teaching Assistant at the Technical University of Sofia, from 1975 to 1987. He has an Associate Professor of television and video technique at Technical University of Sofia, since 1987. His main field of activity is the theoretical study of the television systems, image, sound and signal processing, Matlab Simulation, theory of coding, digital signal processors, digital optical image and signal transmission, coding and processing. He is author or coauthor of 186 papers.

Mariangela Gioannini was born in Cuorgnè, Italy, in 1973. She received the M.S. degree in electronic engineering and the Ph.D. degree in electronic and communication engineering from Politecnico di Torino, Torino, Italy. in 1998 and 2002, respectively.

Since 2002, she has been with the Dipartimento di Elettronica. Politecnico di Torino, first with a post-doctoral position and then as permanent Researcher since January 2005. She was a Visiting Researcher at the Univesity of Bristol, Bristol, U.K. in 2001 and at the Fraunhofer Institut für Nachrichtentechnik, Heinrich-Hertz-Institut, Berlin, Germany, in 2001 and 2002. Her research interests involve modeling and characterization of semiconductor lasers and optical amplifiers. Since 2002, her main research activity has been focused on modelling of quantum-dot and quantum-dash materials, lasers, and optical amplifiers.

Slimane Loualiche was born in Ouacif, Algeria, in 1950.

He is a Full Professor of Optoelectronics at the Institut National des Sciences Appliquées (INSA), Rennes, France, and Head of the LENS. His main field of activity is the experimental and theoretical study of the optical and dynamical properties of QW and QD structures, using in particular fourier transform absorption and pump & probe techniques. He also has a long experience in the epitaxial growth, characterization, and modeling of the properties of nanostructures (QW and QD) and devices. He is author or coauthor of more than 160 scientific papers and of 11 patents.